

# Effect of Ge Additive on the Morphological and Physical Properties of $\text{Se}_{100-x}\text{Ge}_x$ ( $x = 0, 1, 2, 4, 6, 10, 15$ and $20$ ) Chalcogenide System

Anjali<sup>1,a</sup>, Balbir Singh Patial<sup>2,b</sup>, Vaishnav Kiran<sup>1,c</sup> and Nagesh Thakur<sup>2,d</sup>

<sup>1</sup> School of Basic and Applied Sciences, Himachal Pradesh Technical University, Hamirpur-177001, H.P., India.

<sup>2</sup> Department of Physics, Himachal Pradesh University Summerhill Shimla-171005, H.P., India.

<sup>a</sup> [atshpu12@gmail.com](mailto:atshpu12@gmail.com)

<sup>b</sup> [bspatial@gmail.com](mailto:bspatial@gmail.com)

<sup>c</sup> [vaishnav.rana5@gmail.com](mailto:vaishnav.rana5@gmail.com)

<sup>d</sup> [ntb668@yahoo.co.in](mailto:ntb668@yahoo.co.in)

## Abstract

Ge additive chalcogenide materials have become more prevalent in contemporary optoelectronics. The present study utilizes the melt-quenching process for preparing Se-Ge chalcogenide glasses. For the examined system, submicron structural and physical characteristics are examined and described. X-ray diffraction spectra show no characteristic peaks, indicate that the glassy compositions under investigation are amorphous. A further confirmation of the amorphous nature is provided by SEM. The physical properties of the compositions under examination namely cross-linking density ( $X$ ), average coordination number ( $\langle r \rangle$ ), lone-pair electrons ( $L$ ), mean bond energy ( $\langle E \rangle$ ), constraints ( $N_c$ ), fraction of floppy modes ( $f$ ), cohesive-energy ( $CE$ ), glass transition temperature ( $T_g$ ), electro-negativity ( $\chi$ ) as well as heat of atomization ( $H_s$ ) have been deduced in regard to influence of Ge content. Cohesive-energy is computed using CBA approach, while mean bond energy is obtained by chemical-bond ordering approach. Shimakawa's relationship is utilized to compute band gap of the system under investigation theoretically. Average single-bond energy, electro-negativity and cohesive-energy were used to analyse the results. A relationship between the mean coordination number and the inferred physical characteristics is established.

**Keywords:** XRD, SEM, Chalcogenide Glasses, Average Coordination Number, Band Gap, Cohesive-energy, Mean Bond Energy.

Received 29 January 2025; First Review 19 March 2025; Accepted 19 March 2025.

## \* Address of correspondence

Balbir Singh Patial  
Department of Physics, Himachal Pradesh  
University Summerhill Shimla-171005, H.P.  
India.

Email: [bspatial@gmail.com](mailto:bspatial@gmail.com)

## How to cite this article

Anjali, Balbir Singh Patial, Vaishnav Kiran and Nagesh Thakur, Effect of Ge Additive on the Morphological and Physical Properties of  $\text{Se}_{100-x}\text{Ge}_x$  ( $x = 0, 1, 2, 4, 6, 10, 15$  and  $20$ ) Chalcogenide System, J. Cond. Matt. 2025; 03 (01): 106-111.

Available from:

<https://doi.org/10.61343/jcm.v3i01.95>



## Introduction

Glasses and other amorphous materials have a long history that predates nearly all human civilizations. These materials were utilised in pottery and as decoration supplies. Numerous attempts were undertaken at various times to explore the specific characteristics of these materials. On the basis of the absence of long-range order these materials were believed to be non-semiconductors [1]. Without the standardization of different techniques, the results obtained by different research groups happened to be quite divergent [2]. These factors prohibited the development and the proper understanding in this field. During 1950s this field again attracted the interest of researchers due to the groundbreaking work in the experimental sector [3]. Since then, this field has become the central field of research. This field is now acknowledged as being technologically

sensitive. These materials have been found to have a number of remarkable characteristics, including switching, photoconductive, memory retention and semiconducting qualities [2-4]. Chalcogenide glasses have potential and current applications in infrared (IR) lasers, photonic crystals, transistors, optical memories, and IR transmitting optical fibres because of their thermal and optical properties, that depend on composition [5-6]. Chalcogenide materials are being developed for rewritable optical memory [7]. It is necessary to have precise understanding of these material's optical constants across a broad spectrum in order to effectively use them in reflecting coatings and optical fibres. The electrical, electronic band and atomic structures of these material's influence optical characteristics [8]. Because of commercial application and technological significance, Se-based glasses remain quite popular among all chalcogenide systems. These glasses are

appealing because of their special ability to undergo reversible transformation, which has numerous device applications [9].

Even though Se is excellent for glass forming, it has drawbacks including a short lifespan and low sensitivity [10]. Alloying Se with impurity atoms like Te, Ge, Ga, As etc. may resolve these issues [11]. When Ge replaces Se,  $\text{Se}_8$  ring structure is broken, the chain fraction is marginally increased, but chain length decreases [12]. Since Ge improves stability, optical qualities, corrosion resistance, xerography and chemical durability of chalcogenide glassy semiconductors, Ge is chosen as an additive in Se [12]. Ge-doped glasses are emerged as desirable materials for basic studies of their structure and characteristics. Alterations in composition result in short-range order alterations, which are useful for modifying glassy material's features to fulfil particular needs [13]. Additionally, assessing physical factors helps to identify the system's features and can more accurately predict a glassy system's stability, which facilitates problem identification and resolution prior to experimentation.

This study examines the submicron structural characteristics and general physical characteristics of Ge doped  $\text{Se}_{100-x}\text{Ge}_x$  ( $x = 0, 1, 2, 4, 6, 10, 15$  and  $20$  at. wt.%) chalcogenide alloys primed using the melt-quench method. The amorphous nature of the composition under examination and its surface appearance is examined via the XRD and SEM methodology. A relationship between the mean coordination number and the deduced physical parameters is established.

## Experimental Details

The process of melt quenching is utilised to prime bulk samples of  $\text{Se}_{100-x}\text{Ge}_x$  ( $x = 0, 1, 2, 4, 6, 10, 15$  and  $20$  at. wt.%). After being weighed based on their atomic percentages, at a vacuum of around  $\sim 2 \times 10^{-5}$  mbar, 5N extremely pure materials (99.999%) are sealed in a quartz ampoule that is 12 mm in diameter and 5 cm long. A furnace is used to elevate the temperature of the sealed ampoules to  $900^\circ\text{C}$  at pace of  $3\text{--}4^\circ\text{C}$  per minute. For 24 hours at maximum temperature, ampoules are rocked repeatedly to ensure a uniform melt. Rapid quenching is carried out in the ice-cooled water to avoid crystallisation. Then ingots of glassy materials have been removed by breaking the ampoules. A fine powder is made by grinding these ingots. Structural analysis is done at room temperature using the PANalytical X'Pert x-ray diffractometer source, which is equipped with a Ni filtered using Cu  $K\alpha$  ( $\lambda = 1.54056$ ) radiation as X-ray, to take the x-ray diffraction pattern of the examined samples at room temperature in the range  $10^\circ < 2\theta < 90^\circ$  at a scanning rate of  $1^\circ/\text{min}$ . Figure 1 shows XRD spectra of  $\text{Se}_{96}\text{Ge}_4$  chalcogenide alloy under

investigation. The absence of identifiable sharp peaks in the x-ray diffraction spectra indicates that the chalcogenide alloy under investigation is amorphous. For other samples, similar outcomes are realised. Surface morphology and amorphous nature of examined system is further analysed by SEM (QUANTA FEG 250) operating at accelerating voltage of 15 kV; which indicates good consistency with XRD outcomes. The scanned image of  $\text{Se}_{96}\text{Ge}_4$  chalcogenide alloy is displayed in Figure 2. Amorphous character of primed chalcogenide alloy is indicated by SEM image, which clearly illustrates phase separation in the scanned area of the material due to inhomogeneity in the sample. Other samples also yield similar results.

## Results and Discussion

### Average Coordination Number and Constraints

The average coordination number was first used with binary alloys by Phillips and further developed it to characterize characteristics of covalent chain forming quaternary glasses [14]. The formula mentioned below is used to obtain average coordination number  $\langle r \rangle$  for the compound  $\text{Se}_{100-x}\text{Ge}_x$  ( $x = 0, 1, 2, 4, 6, 10, 15$  and  $20$  at. wt.%):

$$\langle r \rangle = \frac{\alpha N_{\text{Se}} + \beta N_{\text{Ge}}}{\alpha + \beta} \quad (1)$$

where  $\alpha$  and  $\beta$  are respective at.wt. % of Se, Ge and  $N_{\text{Se}}$ ,  $N_{\text{Ge}}$  denote their corresponding coordination numbers. Table 1 provides computed  $\langle r \rangle$  values. The  $\langle r \rangle$  was found to be in the range of 2 to 2.40 (Table 1), indicating that  $\langle r \rangle$  rises as Ge content rises. It demonstrates that as the Ge content rises, chains between the atoms are becoming more cross-linked.

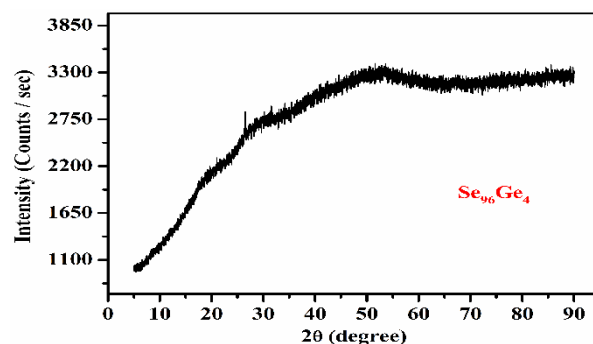
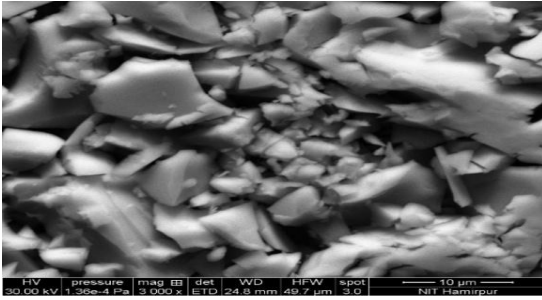


Figure 1: XRD pattern of  $\text{Se}_{96}\text{Ge}_4$  chalcogenide system.

Phillips, Thorpe along with Tanaka established topological limits 2.4 and 2.67, which are commonly recognised as mechanical as well as chemical thresholds, in context of constraint theories. Glasses of chalcogenides with  $\langle r \rangle = 2.4$  are under constrained or weakly connected, whereas those with  $\langle r \rangle = 2.67$  are over constrained or strongly

**Table 1:** Values of  $\langle r \rangle$ ,  $N_a$ ,  $N_\beta$ ,  $N_c$ ,  $f$  and  $X$  for amorphous  $\text{Se}_{100-x}\text{Ge}_x$  ( $x = 0, 1, 2, 4, 6, 10, 15$  and  $20$  at. wt. %).

Composition	$\langle r \rangle$	$N_a$	$N_\beta$	$N_c$	$f$	$X$
$\text{Se}_{100}$	2.00	1.00	1.00	2.00	0.333	0.00
$\text{Se}_{99}\text{Ge}_1$	2.02	1.01	1.04	2.05	0.316	0.05
$\text{Se}_{98}\text{Ge}_2$	2.04	1.02	1.08	2.10	0.300	0.10
$\text{Se}_{96}\text{Ge}_4$	2.08	1.04	1.16	2.20	0.266	0.20
$\text{Se}_{94}\text{Ge}_6$	2.12	1.06	1.24	2.30	0.233	0.30
$\text{Se}_{90}\text{Ge}_{10}$	2.20	1.10	1.40	2.50	0.166	0.50
$\text{Se}_{85}\text{Ge}_{15}$	2.30	1.15	1.60	2.75	0.083	0.75
$\text{Se}_{80}\text{Ge}_{20}$	2.40	1.20	1.80	3.00	0.000	1.00

**Figure 2:** SEM micrograph of  $\text{Se}_{96}\text{Ge}_4$  chalcogenide alloy.

coupled [13]. The structural changes from a two-dimensional network to a three-dimensional network takes place at the chemical threshold of  $\langle r \rangle = 2.67$ . Stiffness percolation limit, for which  $\langle r \rangle = 2.4$  has been projected to be the greatest inclination for glass formation. There are two restrictions for mechanical constraints. Bond stretching constraints per atom are denoted by  $N_a = \langle r \rangle / 2$  while bond bending constraints per atom on a network are denoted by  $N_\beta = 2\langle r \rangle - 3$ . Angular and radial stresses, respectively, cause  $N_\beta$  and  $N_a$  to emerge in covalently bonded glasses. Consequently, sum of  $N_a$  and  $N_\beta$  equals to the total number of mechanical constraints per atom ( $N_c$ ), which is  $N_c = N_a + N_\beta$ .

According to M. F. Thorpe [15], standard modes of vibration at zero frequency or "floppy modes" make up a finite proportion of uncoordinated networks, which can be computed using the following relationship:

$$f = 2 - \frac{5}{6}\langle r \rangle \quad (2)$$

The density of cross-linking is determined using [15]:

$$X = N_c - 2 \quad (3)$$

Table 1 lists determined outcomes for  $N_c$ ,  $f$  along with  $X$  as well as plotted in Figure 3. Figure 3 yields the conclusion that value of  $N_c$  and  $X$  rise as Ge content rises. The ideal circumstance for glass production, as stated by Phillips & Thorpe [16], is when  $N_c$  equals degree of freedom  $N_d$  or  $N_c = N_d = 3$ .  $N_c \rightarrow 3$  with the increase in Ge content shows that degree of freedom available to the atoms in network stabilizes number of constraints ( $N_c$ ) in network.

Additionally, the value of  $f \rightarrow 0$  appears (Table 1). It shows a phase shift from floppy to rigid, and as a result the system becomes increasingly rigid; indicating a stronger propensity for glassmaking in the studied system.

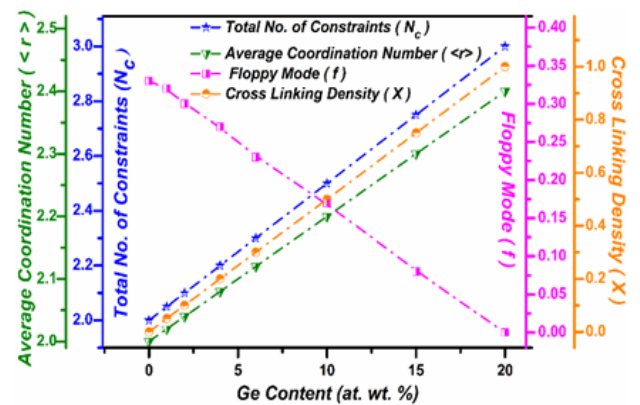
### Glass Forming Ability and Lone Pair Electrons

The valence band contains a single pair of electrons ( $L$ ), which is a non-bonding pair of electrons. If there is a sufficient amount of  $L$  in the chalcogenide system, vitreous state is stable. Given that non-bonding electrons can establish chemical bonds and these bonds are naturally flexible [17]. Therefore, by eliminating strain tension from the system, lone-pair electron occurrence promotes the creation of glass. The following relation was put forth by Phillips [17] to calculate  $L$  in a semiconducting chalcogenide system:

$$L = V - \langle r \rangle \quad (4)$$

where valence electrons are indicated by  $V$ . In order to assess the glass-forming ability of chalcogenide glasses, Zhenhua [18] proposed a straightforward criterion that states that  $L$  should be more than 2.6 for binary systems and greater than 1 for ternary systems. Table 2 lists the computed values of  $L$  and Figure 4 illustrates how they vary with the Ge additive. It illustrates how the Ge content causes  $L$  to decrease. The interaction between the lone pair electrons of the bridging Se atom and the Ge ion can be used to explain the decrease in  $L$ .  $L$  reduced as a result of this systemic interaction. Since values of  $L$  for the system under investigation are found to be more than three, the composition in under investigation has a good propensity to form glass.

### Stoichiometry Deviation, Mean Bond Energy and Glass Transition Temperature

**Figure 3:** Variation of average coordination number ( $\langle r \rangle$ ), total number of constraints ( $N_c$ ), cross-linking density ( $X$ ) and floppy modes ( $f$ ) for amorphous  $\text{Se}_{100-x}\text{Ge}_x$  ( $x = 0, 1, 2, 4, 6, 10, 15$  and  $20$  at. wt. %) chalcogenide system.

$R$  is quantity that represents deviation from stoichiometry and is defined as ratio of chalcogen atoms covalent bonding

assumptions to those of non-chalcogen atoms [13]. Only hetero-polar bonds form at threshold,  $R = 1$ . If  $R > 1$ ; composition is considered chalcogenide rich. If  $R < 1$ ; the composition is deemed chalcogen deficient. The following relationship is used to determine  $R$ :

$$R = \frac{\alpha \times N_{\text{Se}}}{\beta \times N_{\text{Ge}}} \quad (5)$$

Plotting the calculated values of  $R$  in Figure 4 (Table 2) reveals that  $R > 1$  for the composition under investigation. Therefore, it seems that the system being studied is rich in chalcogen. Glassy system features are directly linked to bond energy, average coordination number, degree of cross linking and bond type. Using the correlation provided by Ticha et. al. [19], bond energy  $\langle E \rangle$  evaluated for composition under examination as:

$$\langle E \rangle = E_{cl} + E_{rm} \quad (6)$$

where  $E_{rm}$  represents contribution from weaker bonds that have maximised contribution from strong bonds and  $E_{cl}$  indicates overall participation to bond energy caused by strong hetero-polar bonds.

$$E_{cl} = P_r D_{hb} \quad (7)$$

$P_r$  stands for degree of cross linking and  $D_{hb}$  for average energy of a hetero-polar bond. Table 2 summaries estimated values of  $\langle E \rangle$  and shows that  $\langle E \rangle$  rises as Ge is added. The system's bond energy increases when Ge substitutes Ge-Se heteropolar bonds (49.44 kcal/mol) for Se-Se homopolar bonds (44 kcal/mol) in the system under investigation [12-13].

A transition occurs at the glass transition temperature ( $T_g$ ) and below  $T_g$ , a supercooled liquid turns into a glass. It follows that cohesive forces within material should be overcome in order to permit atomic movement and that their size is proportional to  $T_g$ . A lot of focus is placed on predicting  $T_g$  in chalcogenide glasses, which is correlated with  $\langle E \rangle$ , which indicates both cohesive forces and material stiffness.

Tichy and Ticha have been linked  $T_g$  with  $\langle r \rangle$  and  $\langle E \rangle$  the [20]. They provided following correlation between  $T_g$  and  $\langle E \rangle$  and were regarded as covalent bond approach for chalcogenide systems:

$$T_g = 311[\langle E \rangle - 0.9] \quad (8)$$

Figure 4 shows rise in  $T_g$  with the increase in Ge concentration and values of  $T_g$  derived from Tichy-Ticha are listed (Table 2).  $T_g$  increases when Ge substitutes Ge-Se heteropolar bonds (49.44 kcal/mol) for Se-Se homopolar bonds (44 kcal/mol) in system under investigation [12-13].

#### Average Heat of Atomization, Average Single Bond

#### Energy and Theoretical Band Gap

Average heat of atomization ( $\overline{H}_s$ ) is a metric that indicates relative bond strength of material. When all of the atoms in a chemical substance are completely separated leads to a change in heat [21]. The average non-polar bond energy of the two atoms is related to the sum of the heat of formation ( $\Delta H$ ) and the average heats of atomization  $H_s^A$  and  $H_s^B$  for binary semiconductors made up of A and B atoms at standard pressure and temperature [13]:

$$H_s(A-B) = \Delta H + \frac{1}{2} [H_s^A + H_s^B] \quad (9)$$

The square of the difference in the electro-negativity  $\chi_A$  and  $\chi_B$  of two atoms is associated with the  $\Delta H$  term as:

$$\Delta H \propto (\chi_A - \chi_B)^2 \quad (10)$$

For higher order semiconducting systems, this relation might be extended.  $\overline{H}_s$  is a direct measure of cohesive-energy that may be represented as follows for a quaternary binary system  $\text{Se}_\alpha\text{Ge}_\beta$ :

$$\overline{H}_s = \frac{\alpha H_s^{\text{Se}} + \beta H_s^{\text{Ge}}}{\alpha + \beta} \quad (11)$$

Here  $H_s(\text{Se}) = 227 \text{ kJ/mol}$  and  $H_s(\text{Ge}) = 377 \text{ kJ/mol}$  [12-13]. Table 3 tabulates the obtained values of  $\overline{H}_s$  and  $\overline{H}_s / \langle r \rangle$ . Figure 5 shows the change in  $\overline{H}_s / \langle r \rangle$  with Ge. The binding strength is shown by  $\overline{H}_s / \langle r \rangle$ . As the concentration of Ge increases, it is evident from Figure 5 and Table 3 that  $\overline{H}_s / \langle r \rangle$  decreases at the same time. The substitution of Ge-Se bonds (bond energies 49.44 kcal/mol) for Se-Se bonds (bond energies 44 kcal/mol) may be the cause of decrease in  $\overline{H}_s / \langle r \rangle$  [12-13].

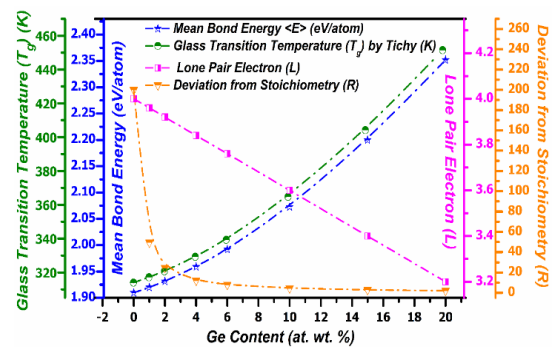


**Figure 4:** Variation of  $L$ ,  $R$ ,  $\langle E \rangle$  and  $T_g$  (K) for examined chalcogenide system.

**Table 2:** Values of  $L$ ,  $R$ ,  $\langle E \rangle$  and  $T_g$  (K) for examined chalcogenide system.

Composition	$L=V-<r>$	$R$	$\langle E \rangle$ eV/atom	$T_g(\text{K})$ by Tichy- Ticha
$\text{Se}_{100}$	4.00	200	1.91	314.02
$\text{Se}_{99}\text{Ge}_1$	3.96	49.5	1.92	317.16
$\text{Se}_{98}\text{Ge}_2$	3.92	24.5	1.93	320.77
$\text{Se}_{96}\text{Ge}_4$	3.84	12.0	1.96	329.32
$\text{Se}_{94}\text{Ge}_6$	3.76	7.83	1.99	339.33
$\text{Se}_{90}\text{Ge}_{10}$	3.60	4.50	2.07	364.75
$\text{Se}_{85}\text{Ge}_{15}$	3.40	2.83	2.20	404.19
$\text{Se}_{80}\text{Ge}_{20}$	3.20	2.00	2.35	451.47

Using Shimakawa correlation [22], the energy gap ( $E_g^{\text{th}}$ ) for Se-Ge glassy composition is calculated theoretically and is as follows:

$$E_g^{\text{th}}(\text{Se} - \text{Ge}) = \alpha E_g(\text{Se}) + \beta E_g(\text{Ge}) \quad (12)$$

where  $E_g(\text{Se}) = 1.95 \text{ eV}$  and  $E_g(\text{Ge}) = 0.95 \text{ eV}$  are the braced element's energy gaps. The fluctuation of  $\overline{H}_s / <r>$  with Ge content is shown in Figure 5. Ge addition reduces the energy gap in the studied Se-Ge system, which can be explained by a correlation between the energy gap and the system bond strength. With the addition of Ge, the energy gap ( $E_g^{\text{th}}$ ) also reduces as  $\overline{H}_s / <r>$  lowers. Moreover, the system's reducing  $E_g^{\text{th}}$  can be explained by the electro-negativity ( $\chi$ ) decreasing as Ge at. wt.% increases (Table 3). The anti-bonding band forms bottom of conduction band in a chalcogenide system, whereas lone pair of Se atoms forms top of valence band [13]. The lone pair energy decreases and the valence band shifts towards the energy gap when the electro-negativity of the Se atom ( $\chi = 2.55$ ) is substituted with that of the electronegative Ge atom ( $\chi = 2.01$ ) [13], which may result in a decrease in the energy band gap.

### Cohesive-energy and Electro-negativity

Cohesive-energy in a solid is defined as the energy needed to break every bond among its constituent atoms. Cohesive-energy is evaluated using chemical bond approach (CBA) [13]. The CBA model states that, unless the valence of the atoms is satisfied, hetero-polar bonds form more readily than homo-polar bonds and appears in a series of decreasing bond energies. Bond energies are also additive in nature. By summing the bond energies of each bond expected in system under study, cohesive-energy is calculated as follows:

$$CE = \frac{\sum_i C_i D_i}{100} \quad (13)$$

In this case,  $D_i$  represents energy of associated bonds, while  $C_i$  represents number of predicted chemical bonds.

**Table 3:** Values of  $H_s / <r>$ ,  $H_s$ ,  $E_g^{\text{th}}$ ,  $CE$  and  $\chi$  for investigated Se-Ge chalcogenide system.

Sample	$H_s$	$H_s / <r>$	$E_g^{\text{th}}$	$CE$	$\chi$
$\text{Se}_{100}$	2.14	1.071	1.95	0.440	2.55
$\text{Se}_{99}\text{Ge}_1$	2.16	1.069	1.94	0.442	2.51
$\text{Se}_{98}\text{Ge}_2$	2.18	1.067	1.95	0.443	2.50
$\text{Se}_{96}\text{Ge}_4$	2.21	1.063	1.90	0.445	2.46
$\text{Se}_{94}\text{Ge}_6$	2.25	1.060	1.88	0.447	2.41
$\text{Se}_{90}\text{Ge}_{10}$	2.32	1.054	1.83	0.451	2.32
$\text{Se}_{85}\text{Ge}_{15}$	2.41	1.046	1.77	0.459	2.22
$\text{Se}_{80}\text{Ge}_{20}$	2.49	1.039	1.71	0.467	2.11

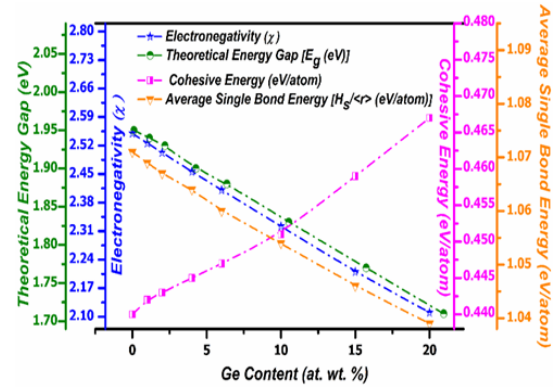


**Figure 5:** Variation of  $H_s / <r>$ ,  $E_g^{\text{th}}$ ,  $CE$  and  $\chi$  with Ge additive for Se-Ge chalcogenide system.

The examined composition's electro-negativity ( $\chi$ ) has been determined via Sanderson's method [23].

The system's electro-negativity ( $\chi$ ) can be represented as the geometric mean of the electro-negativity of its component elements in accordance with Sanderson's hypothesis [23]. The electro-negativity values for Se and Ge are 2.55 and 2.01 respectively on the Pauling scale [12-13]. Figure 5 (Table 3) illustrates how  $CE$  and  $\chi$  change as Ge concentration rises. With content, it has been known that  $CE$  rises and  $\chi$  declines [13]. The decrease in energy gap can be explained by rise in  $CE$ . As a result, a fall in  $CE$  lowers the conduction band edge energy, which in turn lowers the band gap between bonding & anti-bonding orbitals. This results in a reduction of the optical energy gap [13].

### Conclusions

This study examines the submicron structural characteristics and general physical characteristics of Ge-doped Se-Ge chalcogenide alloys prime through melt-quench method. X-ray diffraction patterns show no characteristic peaks, this indicates that glassy compositions under investigation are amorphous. A further confirmation of the amorphous nature is provided by SEM. The inhomogeneity in the samples leads to phase separation in scanned area of SEM micrographs of material. Thus, SEM analysis is consistent with the XRD results. The impact of Ge content has been investigated in theoretical predictions in relation to their physical characterisations using the metrics;  $<r>$ ,  $f$ ,  $\langle E \rangle$ ,  $X$ ,  $L$ ,  $N_c$ ,  $CE$ ,  $H_s$ ,  $\chi$  and  $T_g$ . Cohesive-

energy is computed using CBA, while mean bond energy is obtained by chemical-bond ordering approach. Tichy-Ticha method is used to estimate  $T_g$ . When Ge is added to the Se-Ge system,  $\langle r \rangle$ ,  $N_c$ ,  $X$ ,  $\langle E \rangle$ ,  $CE$ ,  $T_g$  and  $H_s$  are enhanced. However, it is observed that the Ge content decreases  $L$ ,  $f$ ,  $R$ ,  $\chi$  and  $E_g^{\text{th}}$ . This is explained by the fact that as the Ge content increases, Se-Se homopolar bonds (44 kcal/mol) are replaced by Ge-Se heteropolar bonds (49.44 kcal/mol). Shimakawa's relationship was utilized to compute band gap of the system theoretically. Average single-bond energy, electro-negativity and cohesive-energy were used to analyse the results. A relationship between the mean coordination number and deduced physical properties is established.

## References

1. J.M. Ziman. *J. Non-Cryst. Solids*, **4**: 426-427, 1970.
2. A.H. Clark, *Phys. Rev.*, **154**: 750-757, 1967.
3. D.N. Payton and W.M. Visscher. *Phys. Rev.*, **154**: 802-811, 1967.
4. S.C. Moss and J.F. Graczyk. *Phys. Rev. Lett.*, **23**: 1167-1171, 1969.
5. P. Sharma and S.C. Katyal. *Phil. Mag.*, **88**: 2549-2557, 2008.
6. K. Kumar, N. Thakur, S.S. Bhatt and P. Sharma. *Phil. Mag.*, **90**: 3907-3918, 2010.
7. X.H. Zhang, Y. Guimond and Y. Bellac. *J. Non-Cryst. Solids*, **326-327**: 519-523, 2003.
8. E.R. Shaaban. *Phil. Mag.*, **88**: 781-794, 2008.
9. G. Singh, J. Sharma, A. Thakur, N. Goyal, G.S.S. Saini and S.K. Tripathi. *J. Optoelectron. Adv. Mater.*, **7**: 2069-2076, 2005.
10. Anjali, B.S. Patial and N. Thakur. *J. Electron. Mater.*, **51**: 1089-1096, 2022.
11. Anjali, B.S. Patial, S.K. Tripathi and N. Thakur *J. Electron. Mater.*, **46**: 1516-1524, 2017.
12. J. Sharma and S. Kumar. *J. Non-Oxide Glasses*, **1**: 120-130, 2009.
13. Anjali, B.S. Patial and N. Thakur. *J. Asian Ceram. Soc.*, **8**: 777-792, 2020.
14. N. Sharma, B.S. Patial, N. Thakur. *Indian J. Pure Appl. Phys.*, **56**: 128-135, 2018.
15. M.F. Thorpe. *J. Non-Cryst. Solids*, **57(3)**: 355-370, 1983.
16. J.C. Phillips, M. Thorpe, *Solid State Commun.*, **53(8)**: 699-702, 1985.
17. M. Saxena, A.K. Kukreti, S. Gupta, M.K. Agarwal and N. Rastogi. *Arch. Appl. Sci. Res.*, **4**: 994-1001, 2012.
18. L. Zhenhua. *J. Non-Cryst. Solids*, **127(3)**: 298-305, 1991.
19. H. Ticha, L. Tichy, N. Rysava and A. Triska. *J. Non-Cryst. Solids* **74(1)**: 37-46, 1985.
20. L. Tichy, H. Ticha, *Mater. Lett.*, **21(3-4)**: 313-319, 1994.
21. L. Pauling. *J. Phys. Chem.*, **58(8)**: 662-666, 1954.
22. A. Dahshan, K.A. Aly. *Philos. Mag.*, **88(3)**: 361-372, 2008.
23. R.T. Sanderson. *J. Chem. Educ.*, **29(11)**: 539-544, 1952.